Fundamental Investigations of the Free Radical Copolymerization and Terpolymerization of Maleic Anhydride, Norbornene, and Norbornene *tert*-Butyl Ester: In-Situ Mid-Infrared Spectroscopic Analysis

Anthony J. Pasquale,[†] Robert D. Allen,[‡] and Timothy E. Long*,[†]

Department of Chemistry and the Center for Adhesive and Sealant Science, Virginia Polytechnic Institute and State University, Blacksburg, Virginia 24061-0212, and IBM Almaden Research Center, 650 Harry Road, San Jose, California 95120

Received February 12, 2001; Revised Manuscript Received August 13, 2001

ABSTRACT: Various synthetic factors that affect the molecular weight, yield, and composition of maleic anhydride (MAH), norbornene (Nb), and *tert*-butyl 5-norbornene-2-carboxylate (Nb-TBE) terpolymers were investigated. Real-time monitoring via in-situ FTIR spectroscopy of co- and terpolymerizations of MAH with Nb and Nb-TBE was utilized to evaluate the observed rates of varying Nb/Nb-TBE monomer feed ratios. Pseudo-first-order kinetic analysis indicated that the observed rate of reaction (k_{obs}) was a strong function of the Nb/Nb-TBE ratio with a maximum of 6.68×10^{-5} s^{-1} for a 50/0/50 Nb/Nb-TBE/MAH monomer ratio and a minimum of 1.13×10^{-5} s^{-1} for a 0/50/50 Nb/Nb-TBE/MAH ratio. In addition, polymer yields were also observed to be a function of the Nb/Nb-TBE ratio and also decreased with increasing Nb-TBE. Sampling of an Nb/Nb-TBE/MAH (25/25/50 mole ratio) terpolymerization and subsequent analysis using ^{1}H NMR indicated that the relative rate of Nb incorporation is approximately 1.7 times faster than Nb-TBE incorporation. Also, the observed rate constant of 4.42×10^{-5} s^{-1} calculated using ^{1}H NMR agreed favorably with the k_{obs} determined via in-situ FTIR (3.83×10^{-5} s^{-1}). Terpolymerizations in excess Nb-TBE and in the absence of solvent resulted in relatively high molecular weight materials (M_n > 20 000) and provided a potential avenue for control of the Nb/Nb-TBE incorporation into the resulting materials.

Introduction

Photolithography using 193 nm (Ar−F laser) light has emerged for the production of the next generation of microelectronic devices.[1−6] Current technologies (Kr−F laser), including ultraviolet (UV) and deep-UV photolithography, employ aromatic materials based upon phenolic polymers.[7,8] However, the photon energy of 193 nm light is high enough for aromatic polymers to absorb strongly at this wavelength, resulting in opaque materials that are not practical for 193 nm lithography.[9] Therefore, significant attention has been devoted to the design of materials that are optically transparent at 193 nm and also have the desirable etch-resistant and image-forming properties of phenolic-based materials.[10]

A number of approaches to photoresists with high transparency at 193 nm have been reported.[11] Initially, acrylic-based polymers seemed promising as new materials for 193 nm lithography. Acrylates were desirable materials due to only a weak carbonyl absorption at 193 nm, which resulted in good transparency when exposed to this wavelength of light.[12] In 1991, Allen and coworkers described successful 193 nm patterning using an all-acrylic terpolymer composed of methyl methacrylate, *tert*-butyl methacrylate, and methacrylic acid.[13] However, a major disadvantage of acrylic materials was poor reactive-ion etch resistance under the etching conditions used widely in the semiconductor industry.[14] The primary design challenge that has emerged in the development of new materials for 193 nm photolithography is the compromise between imaging performance (broadly defined as resolution, adhesion, sensitivity, and compatibility with industry standard aqueous-base developers) and reactive-ion etch resistance.[10] For the initial acrylic materials, the chemical modifications that were used to tailor imaging performance also deleteriously influenced reactive-ion etch resistance.[14] Previously, it was determined that there is a correlation between increased reactive-ion etch resistance and a high carbon to hydrogen (C/H) ratio.[2,15] This observation supports the fact that phenolic resist materials, which have a high C/H ratio, exhibit good plasma etch resistance. Therefore, an increase in the C/H ratio has resulted in improved reactive-ion etching properties of acrylic-based materials, and a number of acrylic-based materials containing pendant alicyclic adamantane or norbornane substitution have been investigated.[16−22] Incorporation of the pendant alicyclic functionalities greatly improved the etch resistance of acrylic-based materials. However, the increase in etch resistance was also accompanied by decreased image performance. Consequently, 193 nm photolithography acrylic resist materials that possessed both etch resistance and superior image performing properties were not achievable.

An alternative approach to increase the C/H ratio has been to incorporate alicyclic structures directly into the polymer backbone.[12] A variety of synthetic routes for producing resist materials with alicyclic backbones have been investigated. For example, cyclic olefin alternating free radical copolymerization,[22−30] metal-catalyzed vinyl addition polymerization,[23,24,31−33] and ring-opening metathesis polymerization (ROMP) followed by hydrogenation.[23,24] In recent years, the most promising of these methods that has emerged for synthesizing alicyclic materials for 193 nm lithography is the alternating free radical copolymerization of maleic anhydride with cyclic olefin monomers such as norbornene (Scheme 1).[3,6,28]

[†] Virginia Polytechnic Institute and State University.
[‡] IBM Almaden Research Center.

10.1021/ma010257x CCC: $20.00
Published on Web 10/06/2001

Scheme 1. Maleic Anhydride and Norbornene Alternating Copolymerization Scheme

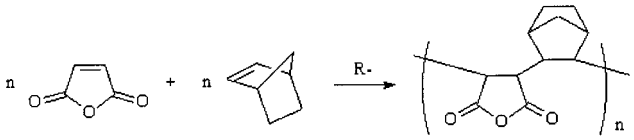

Cyclic olefins will homopolymerize poorly via free radical methods. However, norbornene is a cyclic olefin that contains bridged allylic hydrogens that do not chain transfer to an appreciable extent due to the resulting unstable radical.[34] When norbornene is combined with the electron-poor olefin maleic anhydride in the presence of a free radical initiator, copolymerization occurs in an alternating manner.[3] In addition, maleic anhydride also serves to incorporate polar functionality into the polymer, providing necessary adhesion and solubility properties that are required for imaging performance while retaining sufficient etch resistance in 193 nm resist applications.[28,35,36] The cyclic olefin character of these materials provides for excellent etch resistance, surpassing even currently utilized phenol-based resists. Furthermore, the increased etch resistance is of great importance because of the decreasing film thickness necessary for the achievement of increasingly smaller feature sizes.[3] In addition, the ability to modify the polymer properties via incorporation of cyclic olefin derivatives that improve lithographic performance has resulted in attractive routes to new materials for 193 nm lithography.

Despite the abundance of scientific literature describing the alternating copolymerization of maleic anhydride with electron-rich olefins, multicomponent copolymerizations with norbornene(s) proceed via a complicated polymerization mechanism resulting in the uncontrolled formation of low molecular weight oligomers.[23,28,29] Although these alicyclic copolymers were prepared using a relatively uncontrollable polymerization process, the copolymers were successfully demonstrated as 193 nm imaging materials with improved plasma-etch resistance. Ito and co-workers have recently described an investigation of the copolymerization of norbornene or a *tert*-butyl ester substituted norbornene with maleic anhydride using ^{1}H NMR spectroscopy.[37,38] Monomer consumption studies indicated that copolymerization of a norbornene *tert*-butyl ester with maleic anhydride in dioxane at 84 °C resulted in lower yields (32%) compared to that of norbornene (60%). NMR-scale reactions (<0.08 g total monomer) did not provide optimized copolymerization conditions, comparative rate constants, or molecular weights and molecular weight distributions. In addition, terpolymerizations of norbornene, norbornene *tert*-butyl ester, and maleic anhydride, which more closely exemplify 193 nm microlithographic applications, were not reported. Our research objectives have focused on the investigation of synthetic factors that influence the molecular weight, yield, and composition of terpolymers of maleic anhydride (MAH), norbornene (Nb), and *tert*-butyl 5-norbornene-2-carboxylate (Nb-TBE). This has been achieved using a unique combination of experimental variation, in-situ infrared spectroscopy, and nuclear magnetic resonance spectroscopy. In-situ infrared spectroscopy of alternating copolymerizations has not been reported earlier, and this experimental approach is more facile than conventional NMR approaches. This fundamental understanding will provide the basis for the development of a polymerization system that results in more predictable molecular weights and higher polymerization yields. The development of a fundamental understanding of the polymerization mechanism for maleic anhydride with norbornene and norbornene derivatives will result in viable manufacturing processes and improved 193 nm lithographic performance. In-situ infrared analysis of terpolymerizations containing maleic anhydride, norbornene, and acrylic monomers will also be discussed.

Experimental Section

Materials. All reagents were purchased from Aldrich and used as received unless otherwise noted. Nb-TBE was generously donated by BF Goodrich Co., the preparation of which has previously been reported by Willson et al.[24] Maleic anhydride was purified via sublimation and used immediately. Tetrahydrofuran (THF) was distilled immediately prior to polymerization using the classic sodium/benzophenone ketyl.

Characterization. ^{1}H NMR spectra were obtained using a Varian UNITY 400 spectrometer at 400 MHz in $CDCl_3$ at ambient temperature. ^{13}C NMR spectra were obtained using a Varian UNITY-400 spectrometer at 100 MHz in DMSO-d_6 at ambient temperature. Molecular weights were measured using a miniDAWN multiangle laser light scattering (MALLS) detector with a 690 nm laser (Wyatt Technology, Santa Barbara, CA) connected to a Waters SEC (515 pump, 717 autosampler, and 410 refractive index detector). The miniDAWN was connected in series after three 5-μm Plgel mixed-bed columns (Polymer Laboratories, Amherst, MA). Measurements were made at 40 °C with THF as the solvent at a flow rate of 1.0 mL/min.

In-Situ FTIR. In-situ mid-FTIR spectra were collected with an ASI Applied Systems ReactIR 1000 reaction analysis system equipped with a light conduit and DiComp (diamond-composite) insertion probe. The details and capabilities of the ReactIR 1000 reaction analysis system based on attenuated total reflectance (ATR) have been described in detail previously.[39]

Synthesis and in-Situ FTIR of Nb/Nb-TBE/MAH Terpolymers. A representative synthesis of a Nb/Nb-TBE/MAH terpolymer (Scheme 2) with in-situ FTIR monitoring is described. In a 100 mL, round-bottomed, two-necked flask that was fitted with the ReactIR 1000 DiComp probe was added a magnetic stir bar, Nb (4.79 g, 51 mmol), Nb-TBE (9.89 g, 51 mmol), MAH (10.0 g, 102 mmol), 2,2-azobis(isobutyronitrile) (AIBN) (1.004 g, 6.12 mmol), and THF (16.5 mL). The flask was purged with nitrogen for approximately 1 min and sealed tightly under positive nitrogen pressure (4−5 psi) with a rubber septum. An oil bath at 65 °C was raised to the reaction flask, and FTIR data collection was started. The ReactIR was programmed to collect an FTIR spectrum of the reaction mixture every 5 min. The reaction was then stirred at 65 °C for 24 h while collecting FTIR spectra. The oil bath was removed after 24 h, and the reaction contents were allowed to cool to room temperature. After 24 h, the reaction mixture had solidified to a glass and was no longer stirring. The DiComp probe was removed from the reaction flask, and THF (∼50 mL) was added to dissolve the solid glass. After completely dissolving in THF (approximately 24 h), the dissolved material was precipitated into hexanes (∼500 mL), filtered, washed with isopropyl alcohol (∼200 mL), and dried overnight under vacuum (0.1 mmHg) at approximately 75 °C to give 19.6 g (80% yield) of white powder. GPC: $M_n = 6700$ ($M_w/M_n = 1.64$). Nb/MAH (50/50) copolymer had a 10% weight loss at 355 °C (nitrogen) and a glass transition temperature of 275 °C. A Nb/Nb-TBE/MAH (25/25/50) terpolymer showed a lower 10% weight loss at 220 °C (nitrogen) resulting from degradation of the *tert*-butyl ester functionality.

Results and Discussion

Nb/MAH Free Radical Alternating Copolymerization Reaction Conditions. Research efforts were

Scheme 2. Nb/Nb-TBE/MAH Alternating Terpolymerization Scheme

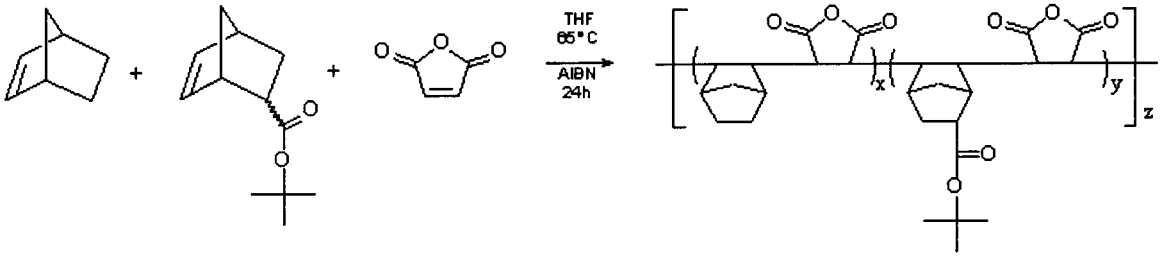

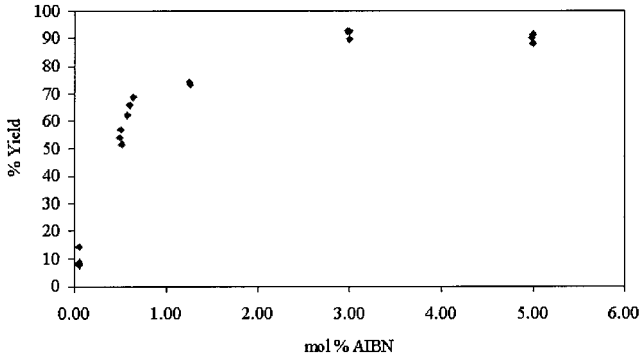

Figure 1. Percent yield vs mol % AIBN (THF, 60% solids, 65 °C, 24 h).

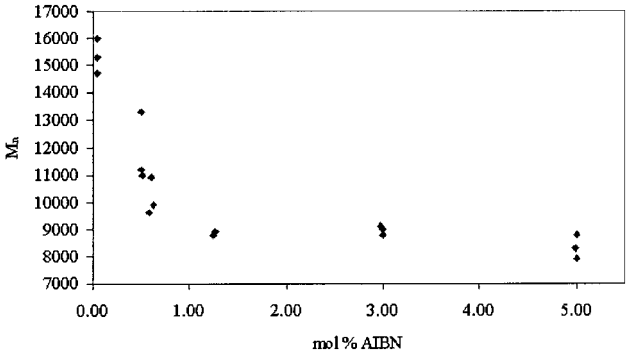

Figure 2. Number-average molecular weight vs mol % AIBN (THF, 60% solids, 50/50 Nb/MAH, 65 °C, 24 h).

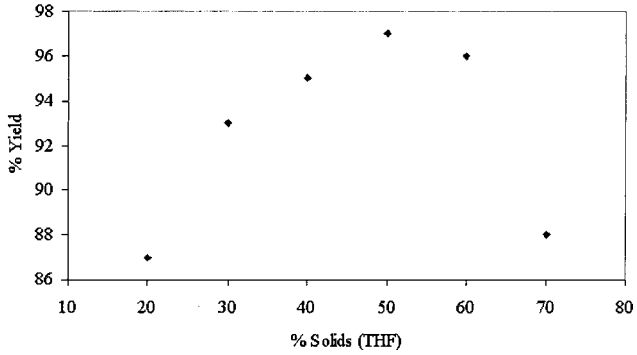

Figure 3. Percent yield vs solids % in THF (3 mol % AIBN, 50/50 Nb/MAH, 65 °C, 24 h).

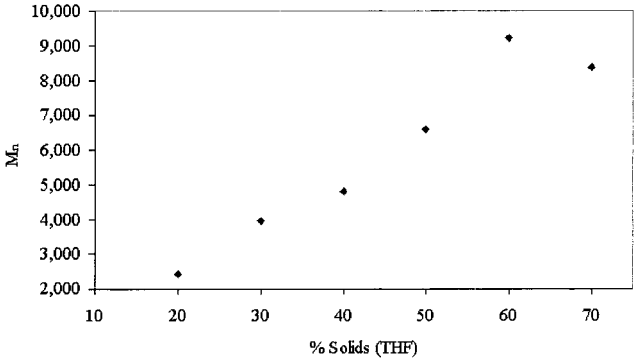

Figure 4. Number-average molecular weight vs solids % in THF (3 mol % AIBN, 50/50 Nb/MA, 65 °C, 24 h).

initially focused on developing an understanding of the factors that influence the copolymerization of norbornene and maleic anhydride polymerization processes. Special attention was devoted to the effects of monomer feed ratio, monomer:solvent ratio, and initiator concentration. In addition, particular focus was also directed toward the development of in-situ infrared spectroscopy techniques for the real time assessment of polymerization kinetics and conversion. It was demonstrated that the monomer feed ratio did not strongly influence the molecular weight and isolated yield in a significant manner, and products with number-average molecular weights ranging from 8000 to 9000 and 80−90% yields were typically obtained. As expected, an increase in initiator concentration resulted in a decrease in the number-average molecular weight; however, a simultaneous increase in yield was also observed (Figures 1 and 2). A maximum in both yield and number-average molecular weight was observed at approximately 50−60% monomer solids in tetrahydrofuran (THF) (Figures 3 and 4). A maximum is attributed to an expected increase in solution viscosity as the polymerization proceeds, and spectroscopic analyses were performed prior to an appreciable increase in the solution viscosity. Kinetic analyses using monomer conversion were based on spectroscopic analysis during the first 4 h of polymerization to ensure the absence of viscosity effects. The following optimum reaction conditions were determined from these initial investigations: equimolar feed ratio Nb and MAH, 3 mol % AIBN (based on total monomer), 60% solids in THF solvent for 24 h at 65 °C.

In-Situ FTIR and Kinetic Analysis of Nb/Nb-TBE/MAH Free Radical Terpolymerization. A derivative of Nb containing a *tert*-butyl ester functionality, Nb-TBE, was also investigated in copolymerizations with MAH and terpolymerizations with Nb and MAH. In free radical copolymerizations with MAH, Nb-TBE behaved similarly to Nb and formed an almost perfectly alternating copolymer with MAH. Terpolymers prepared via free radical polymerization of Nb, Nb-TBE, and MAH (Scheme 2) resulted in multicomponent copolymers that theoretically contained alternating sequences of MAH/Nb and MAH/Nb-TBE. (Monomer consumption studies of terpolymerizations indicated that 50 mol % of converted monomer was MAH.) In-situ infrared spectroscopy provided real-time changes in monomer absorbances and allowed for comparative kinetic analysis of the Nb/Nb-TBE/MAH free radical terpolymerization processes. We have previously utilized in-situ FTIR as a method to study the kinetics of

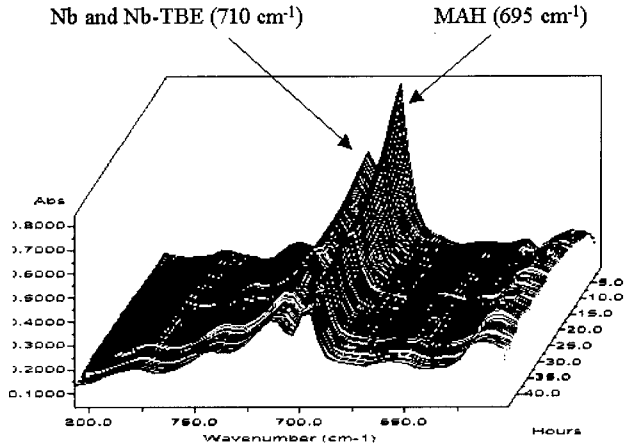

Figure 5. Vinylene region of "waterfall plot" for Nb/Nb-TBE/MAH (25/25/50 mol ratio) terpolymerization (in-situ FTIR, spectrum acquired every 5 min).

stable free radical polymerization (SFRP) processes for linear and star-shaped polystyrene.[40−42] A reaction flask was specifically designed to permit the introduction of the ATR-based infrared probe, and attention was devoted to ensure the reactor was sealed to eliminate any volatilization of reaction components. Strong vinylene (=C−H) absorbances of the monomers were observed and allowed for kinetic analysis of the terpolymerizations using in-situ FTIR. The waterfall plot of the vinylene =C−H region for a Nb/Nb-TBE/MAH (25/25/50 mol ratio) is illustrated in Figure 5. The vinylene absorbances of Nb and Nb-TBE overlapped and were observed at 710 cm^{-1}. The vinylene absorbance of MAH was observed at 695 cm^{-1}. Pseudo-first-order kinetic plots were constructed from the data obtained via the in-situ monitoring of the monomer absorbances. Initial kinetic interpretations have focused on the assumption of pseudo-first-order kinetics for an alternating polymerization mechanism (Figure 6). Excellent agreement was observed using these assumptions, and linear kinetic plots were observed. A representative kinetic plot of ln[monomer absorbance (total area from 670 to 725 cm^{-1})] vs time for a Nb/Nb-TBE/MAH (25/25/50 mol ratio, $k_{obs} = 3.83 \times 10^{-5}\ s^{-1}$) terpolymerization is shown in Figure 7.

Free radical terpolymerizations of Nb/Nb-TBE/MAH with various ratios of Nb to Nb-TBE (while maintaining a 50% molar feed of maleic anhydride) were performed using previously determined optimum conditions (3 mol % AIBN, THF (60% solids), 24 h). Terpolymerizations were conducted using the following Nb/Nb-TBE/MAH monomer feed ratios: 50/0/50, 35/15/50, 25/25/50, 15/35/50, 0/50/50. The observed rate constants determined using in-situ FTIR, percent yields, molecular weights, and Nb/Nb-TBE composition in the resulting materials are summarized in Table 1. Several trends are apparent from the data analysis. First, the observed reaction rate is a strong function of the monomer feed ratio of Nb/Nb-TBE with a maximum of $6.68 \times 10^{-5}\ s^{-1}$ at a 50/0/50 Nb/Nb-TBE/MAH monomer feed ratio. The observed rate decreases with increasing Nb-TBE monomer feed to a minimum of $1.13 \times 10^{-5}\ s^{-1}$ at a 0/50/50 Nb/Nb-TBE/MAH monomer feed ratio. In addition, percent yield exhibits a similar trend with a maximum yield of 94% for a 50/0/50 Nb/Nb-TBE/MAH feed ratio and a minimum yield of 60% observed for a 0/50/50 Nb/Nb-TBE/MAH feed ratio. The observed decrease in rate with increasing Nb-TBE is proposed to be due to a combination of steric and electronic effects resulting from the *tert*-butyl ester functionality of Nb-TBE. Further experiments are planned to elucidate these effects more thoroughly, and current efforts involve the investigation

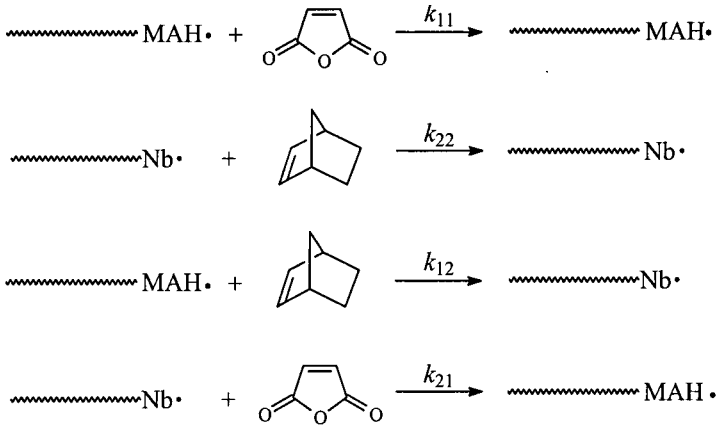

assuming negligible homopolymerization of MAH and Nb, $k_{11}=k_{22}=0$, overall rate is:

$$\text{rate} = k_{12}[(\text{MAH}\cdot)(\text{Nb})] + k_{21}[(\text{Nb}\cdot)(\text{MAH})]$$

assuming a steady state radical concentration and alternating polymerization, rate is:

$$\text{rate} = (k_{12} + k_{21})([\text{P}\cdot][\text{M}])$$

where [P·] = conc. of growing polymer radicals and [M] = conc. of MAH or Nb monomer

and therefore an observed rate constant (k_{obs}) is obtained from a plot of ln[M] vs. time

$$\boldsymbol{k_{obs} = (k_{12} + k_{21})[\text{P}\cdot]}$$

Figure 6. Pseudo-first-order alternating polymerization kinetic assumptions.

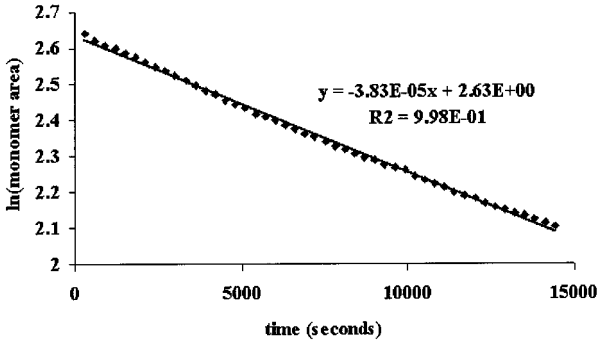

Figure 7. Pseudo-first-order kinetic treatment of convoluted Nb, Nb-TBE, and MAH (total area from 670 to 725 cm^{-1}) absorbances determined via in-situ FTIR.

Table 1. Summary of Nb/Nb-TBE/MAH Terpolymerizations Varying the Monomer Feed Ratio of Nb to Nb-TBE

Nb/Nb-TBE/ MAH	obsd rate (FTIR) $\times 10^5$ s^{-1} [a]	yield (%)	M_n [b]	M_w/M_n	Nb/Nb-TBE [c]
50/0/50	6.68	94	7300	1.63	
35/15/50	5.26	87	6500	1.46	3.2
25/25/50	3.83	80	6700	1.64	1.4
15/35/50	2.61	75	6600	1.49	0.68
0/50/50	1.13	60	6900	1.59	

[a] Determined from first-order kinetic plot using MAH/NB peak area via in-situ FTIR for first 4 h of reaction. [b] Wyatt miniDAWN MALLS detector coupled with Waters GPC with external 410 RI detector viscometer, THF solvent at 40 °C, and 1.0 mL/min flow rate. [c] Determined using ^{13}C NMR (Varian Unity-400) at 100 MHz, DMSO-d_6, ambient temperature. Ratio calculated from integration of the quaternary carbon of *tert*-butyl ester group (δ 80 ppm) of Nb-TBE to the total carbonyl region (δ 170−176 ppm). For calculation, a 1:1 ratio of MAH to total cyclic olefin (Nb and Nb-TBE) is assumed.

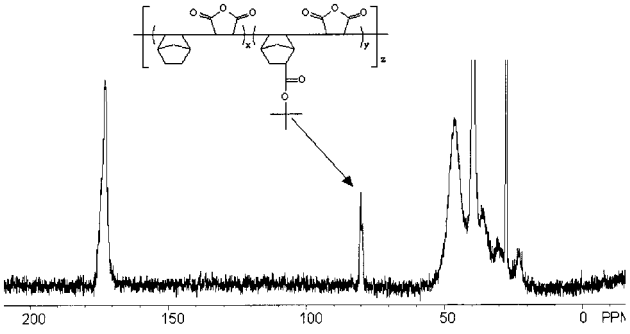

Figure 8. ^{13}C NMR (DMSO-d_6) spectra of terpolymer prepared from a 25/25/50 Nb/Nb-TBE/MAH monomer feed ratio.

of additional Nb monomers containing other electron-withdrawing groups such as the cyano and methyl ester derivatives. ^{13}C NMR analysis of terpolymers prepared from a 25/25/50 Nb/Nb-TBE/MAH monomer feed ratio further indicated that the terpolymers were enriched in Nb and depleted in Nb-TBE. The ^{13}C NMR spectrum of a Nb/Nb-TBE/MAH terpolymer is illustrated in Figure 8. The results obtained using ^{13}C NMR are quantitative based upon a carbon relaxation time experiment that was performed to calibrate the recycle delay for a Nb-TBE/MAH copolymer. The ratio of Nb to Nb-TBE in the terpolymer was subsequently determined via integration of the quaternary carbon of *tert*-butyl group (δ 80 ppm) to the carbonyl region (δ 170−176 ppm). Assuming a 1:1 molar ratio of MAH to the total cyclic olefin (Nb and Nb-TBE) incorporated into the terpolymer, the ratio of Nb to Nb-TBE incorporated was subsequently determined to be 1.4:1.0 and confirmed that the final polymer composition does not match the monomer feed.

Sampling and ^1H NMR Analysis. In parallel with in-situ real-time monitoring, a 25/25/50 Nb/Nb-TBE/MAH terpolymerization was sampled with time and subsequently analyzed using ^1H NMR at regular intervals for the first 8 h. ^1H NMR was a useful method for the spectroscopic separation of the norbornene and norbornene ester monomers. In addition, this technique was used to compare and evaluate the utility of in-situ FTIR. The ^1H NMR spectrum depicting olefinic proton assignments for maleic anhydride, norbornene, and norbornene ester is shown in Figure 9. Moreover, it was determined using ^1H and ^{13}C NMR that the norbornene ester is a mixture of approximately 74% endo and 26% exo stereoisomers. The assignments for the exo and endo stereoisomers are also shown in Figure 9. It is important to note that the ratio of endo to exo isomers did not change within the error of the NMR instrument and was approximately 74/26 throughout the entire polymerization, indicating that neither isomer shows a preference toward polymerization. Ito et al. have also observed that neither the exo nor endo isomers of Nb-TBE show a preference toward polymerization with maleic anhydride under free radical conditions.[37] In contrast, Hennis and Sen have recently shown that exo-substituted norbornenes are polymerized more readily than endo-substituted norbornenes via palladium-catalyzed insertion polymerization.[43] It is also expected for conventional free radical polymerization that exo-substituted norbornenes would react faster than endo-substituted norbornenes since endo substitution may sterically hinder the norbornene olefinic site. However, since neither isomer shows preference in the free radical copolymerization with maleic anhydride, it is proposed that the lower reactivity of substituted norbornenes is not due solely to steric factors.

Monomer conversion data are typically obtained from the relative integration of monomer and polymer resonances; however, the ^1H NMR spectra of terpolymers in Table 2 were very broad and unresolved, and this conventional approach was not suitable. Thus, to determine conversion data for the terpolymerizations, the monomer peaks were integrated relative to the THF solvent peak at δ 3.7 ppm. The solvent peak was presumed to remain at the same relative concentration throughout the reaction since the reactions were performed under positive nitrogen pressure, and attention was devoted to ensure that the reactor was sealed tightly to eliminate any volatilization of reaction components. Terpolymerization conversion data obtained using ^1H NMR are summarized in Table 2. First-order kinetic plots constructed from the conversion data of MAH (Figure 10), Nb (Figure 11), and Nb-TBE (Figure 11) were linear and complimented kinetic analysis using in-situ FTIR data. Assuming alternating copolymerization of Nb and Nb-TBE with MAH, first-order kinetic analysis of MAH using ^1H NMR was directly compared to analysis via in-situ FTIR. The value obtained using ^1H NMR (4.42×10^{-5} s^{-1}, Figure 10) correlated well with the value from in-situ FTIR (3.83×10^{-5} s^{-1}, Figure 7). The observed rate constants for both Nb and Nb-TBE (Figure 11) were linear with a ratio in rates of approximately 5:3 (Nb:Nb-TBE). This result combined with complementary kinetic analysis of copolymerizations using in-situ FTIR (Table 1), which showed that the copolymerization of Nb and MAH was approxi-

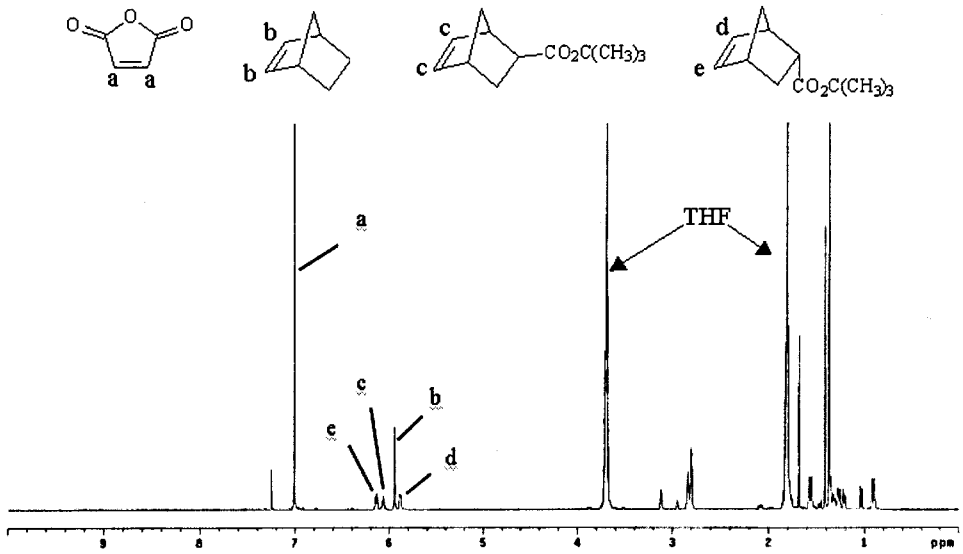

Figure 9. ^{1}H NMR ($CDCl_3$) of Nb/Nb-TBE/MAH (25/25/50 mol ratio) reaction mixture.

Table 2. Conversion Data for a Nb/Nb-TBE/MAH (25/25/50 Mole Ratio) Terpolymerization Determined from ^{1}H NMR Analysis

	conversion (%)[a]		
time (h)	MAH	Nb	Nb-TBE
0	0	0	0
1	28	32	9
2	31	44	18
3	54	51	27
4	50	62	32
5	58	68	39
6	64	73	48
7	71	77	53
8	74	80	58

[a] ^{1}H NMR ($CDCl_3$ solvent).

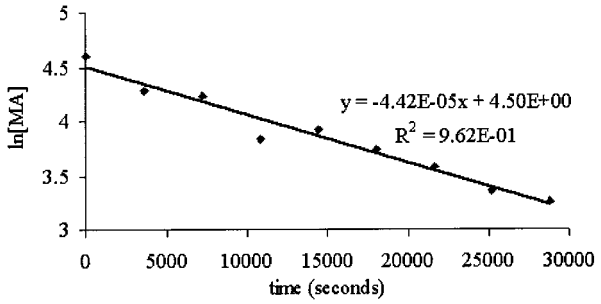

Figure 10. First-order kinetic analysis of maleic anhydride conversion (determined using ^{1}H NMR analysis of samples taken every hour for the first 8 h).

mately 6 times faster than the copolymerization of Nb-TBE and MAH, provides an interesting insight into the reaction mechanism. It was previously discussed that the slower reaction rate of the Nb-TBE olefinic site was likely due to a combination of steric and electronic effects. However, the presence of Nb-TBE in a terpolymerization also decreases the rate of Nb propagation. Future efforts will involve the addition of carbonyl-containing additives to the copolymerization of Nb and MAH in order to ascertain the effect of polar groups on the propagation rate constant for norbornene (Nb).

Nb/Nb-TBE/MAH Terpolymerizations in Excess Nb-TBE and in the Absence of Solvent. This methodology is particularly promising since a bulk polymerization provides an economical and environmentally friendly route for these terpolymeriztions. Furthermore,

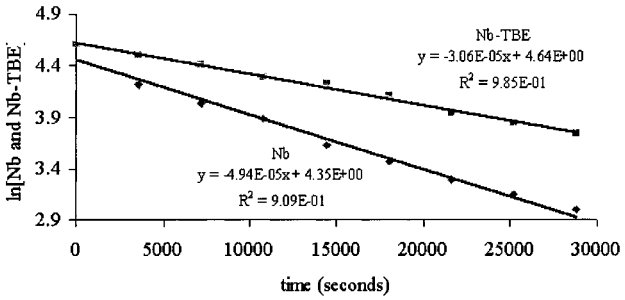

Figure 11. First-order kinetic analysis of Nb and Nb-TBE conversion (determined using ^{1}H NMR analysis of samples taken every hour for the first 8 h).

Table 3. Effect of Excess Nb-TBE on the Terpolymerization Process

excess Nb-TBE	yield (%)	M_n[a]	M_w/M_n	Nb/Nb-TBE[b]
1× Nb-TBE	53	20 200	1.54	1.50
2× Nb-TBE	85	20 000	1.56	0.66
4× Nb-TBE	91	17 100	1.53	0.22

[a] Wyatt miniDAWN multiple angle laser light scattering detector in-line with Waters GPC system with 410 RI detector, 40 °C, and 1.0 mL/min. [b] Determined using ^{13}C NMR (Varian Unity-400) at 100 MHz, DMSO-d_6, ambient temperature. Ratio calculated from integration of the quaternary carbon of *tert*-butyl ester group (δ 80 ppm) of Nb-TBE to the total carbonyl region (δ 170−176 ppm). For calculation, a 1:1 ratio of MA to total cyclic olefin (Nb and Nb-TBE) is assumed.

performing the terpolymerizations in excess Nb-TBE offers the potential to control the incorporation of Nb-TBE into the terpolymers. All reactions were allowed to proceed for 24 h at 65 °C. The results of the experiments are summarized in Table 3. The excess of Nb-TBE to Nb was varied while maintaining a 1:2 molar charge of Nb to MAH. As one can see in Table 3, relatively high molecular weights for these terpolymerizations were obtained using this methodology. Number-average molecular weights close to 20 000 were obtained when the polymerization was performed in excess Nb-TBE compared to number-average molecular weights consistently around 7000 when the terpolymerizations are performed in THF solvent at 60% solids. In addition, it was observed that the Nb/Nb-TBE ratio in the terpolymers was controllable via changing the excess amount of Nb-TBE in the monomer feed. The Nb/Nb-

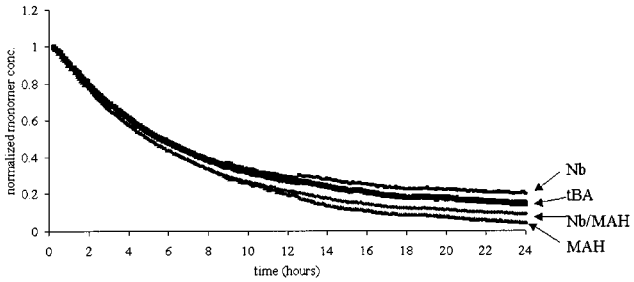

Figure 12. Normalized monomer concentrations for a 50/50/15 Nb/MAH/tBA terpolymerization determined via in-situ FTIR.

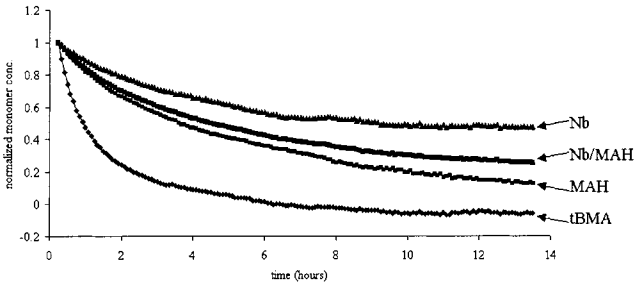

Figure 13. Normalized monomer concentrations for a 50/50/15 Nb/MAH/tBMA terpolymerization measured via in-situ FTIR.

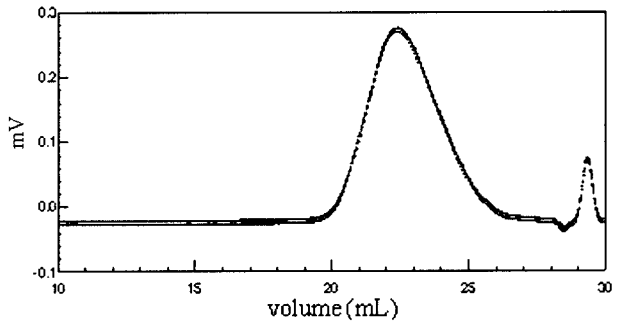

Figure 14. GPC chromatogram of 50/50/15 Nb/MAH/tBA terpolymerization.

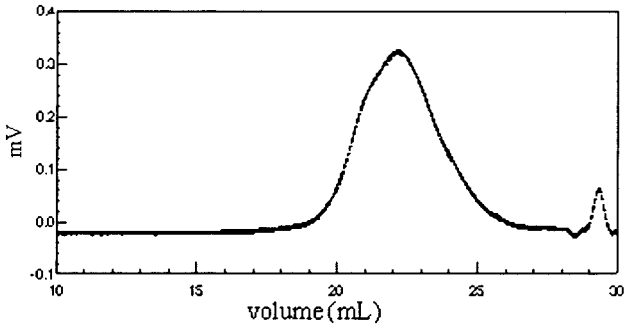

Figure 15. GPC chromatogram of 50/50/15 Nb/MAH/tBMA terpolymerization.

TBE ratio in the terpolymer decreased from a maximum of 1.50 using a 1:1 Nb:Nb-TBE monomer feed ratio to 0.22 using a 1:4 Nb:Nb-TBE monomer feed ratio (Table 3). Preliminary in-situ infrared analysis of the terpolymerizations in excess Nb-TBE were complicated due to absorbance overlap.

Nb/MAH Copolymerizations with the Addition of *tert*-Butyl Acrylate (tBA) and *tert*-Butyl Methacrylate (tBMA). The addition of tBA and tBMA to copolymerizations of Nb and MAH was also studied. Previously, Reichmanis and co-workers have reported that tBA (up to 0.3 mole fraction) can be incorporated in a controlled and predictable manner into free radical alternating copolymerizations of Nb and MAH.[28] In-situ FTIR was used to follow and evaluate monomer conversion for 50/50 Nb/MAH copolymerizations incorporating 15 mol % (based upon total Nb and MAH concentration) of either tBA or tBMA. The remaining reaction conditions were based upon previously optimized conditions (3 mol % AIBN, THF, 60% solids, 65 °C for 24 h under positive nitrogen pressure (5−10 psi)). Normalized monomer conversions that were determined real-time via in-situ FTIR are illustrated in Figures 12 and 13. Conversion values were based upon FTIR absorbance peak heights corresponding to each monomer. As one can see, the conversion profiles of monomers were significantly different between the reactions incorporating either tBA or tBMA. Although the free radical homopolymerization rate of an acrylate is expected to be approximately 4 times faster than a corresponding methacrylate,[44] tBMA reacted much faster than tBA under identical conditions in these systems. In addition, the conversion of Nb and MAH was disrupted more in the presence of tBMA, and only low conversion of Nb occurred in the reaction with tBMA. This observation agrees well with Ito's earlier efforts;[37] however, molecular weight and molecular weight distribution data were not presented. The yield of the 50/50/15 Nb/MAH/tBA terpolymerization was 83% with a number-average molecular weight of 7800 ($M_w/M_n = 1.74$) using MALLS detection. The 50/50/15 terpolymerization of Nb/MAH/tBMA resulted in a lower yield of 68% with a number-average molecular weight of 11 800 ($M_w/M_n = 1.60$) using MALLS detection. GPC was performed directly on the reaction mixtures after 24 h to ensure the polymers were not fractionated during precipitation. The chromatograms of the terpolymerization reaction mixtures are illustrated in Figures 14 and 15. The chromatogram of the Nb/MAH/tBA terpolymerization (Figure 14) appears to be symmetric and monomodal while the chromatogram of the Nb/MAH/tBMA terpolymerization (Figure 15) is slightly bimodal with a high molecular weight shoulder indicating heterogeneity, which supports further that tBA is incorporated more uniformly than tBMA into free radical alternating copolymerizations of Nb and MAH.

Conclusions

Synthetic factors that affect the molecular weight, yield, and composition of Nb/Nb-TBE/MAH terpolymers have been investigated. Efforts have indicated optimum reaction conditions in terms of yield and molecular weight for free radical alternating copolymerizations of Nb and MAH as follows: 60% solids in THF, 3.0 mol % AIBN compared to total monomer amount, a 50:50 molar ratio of Nb:MAH, and 65 °C for 24 h. Real-time monitoring via in-situ FTIR spectroscopy of alternating terpolymerizations of MAH with Nb and Nb-TBE was utilized to evaluate the relative rates of varying Nb/Nb-TBE monomer feed ratios. Pseudo-first-order kinetic plots constructed from the in-situ FTIR absorbance data indicated that the rate of reaction was a strong function of the Nb/Nb-TBE ratio and decreased with increasing Nb-TBE. Additionally, percent yields were also observed to be a function of the Nb/Nb-TBE ratio and again decreased with increasing Nb-TBE. In addition, sampling of a Nb/Nb-TBE/MAH (25/25/50 mole ratio) terpolymerization and subsequent analysis using ^{1}H NMR

indicated that the relative rate of Nb incorporation was approximately 1.7 (5/3) times faster than Nb-TBE incorporation. Terpolymerizations carried out in excess Nb-TBE in the absence of solvent resulted in higher molecular weights and provided for a relative amount of control of the Nb/Nb-TBE incorporation into the resulting materials. Copolymerizations of Nb and MAH with the addition of tBA or tBMA as a third monomer showed that tBMA reacted much faster than tBA under identical conditions in these systems, and the conversion of Nb and MAH was disrupted more in the presence of tBMA and only low conversion of Nb occurred in the reaction with tBMA.

Acknowledgment. Financial support provided by IBM, Jeffress Memorial Trust, Virginia Tech Department of Chemistry, National Science Foundation (CRIF CHE-9974632), and the Center of Adhesive and Sealant Science (CASS) at Virginia Tech and the Adhesive and Sealant Council (ASC) is gratefully acknowledged. The authors thank Thomas Glass at Virginia Tech for assistance with NMR analysis.

References and Notes

(1) Nozaki, N.; Kaimoto, M.; Takahashi, S.; Takeshi, S.; Abe, N. *Chem. Mater.* **1994**, *6*, 1492.
(2) Kunz, R. R.; Palmateer, A. R.; Forte, A. R.; Allen, R. D.; Wallraff, G. M.; DiPietro, R. A.; Hofer, D. C. *Proc. SPIE—Int. Soc. Opt. Eng.* **1996**, *2724*, 365.
(3) Allen, R. D.; Opitz, J.; Larson, C. E.; Wallow, T. I.; Hofer, D. C. *Microlithogr. World* **1999 (**winter**)**, 5.
(4) Jung, M. H.; Jung, J. C.; Lee, G.; Baik, K. H. *Jpn J. Appl. Phys., Part 1* **1998**, *37*, 6889.
(5) Nalamasu, O.; Houlihan, R. A.; Cirelli, A. G.; Watson, G. P.; Hutton, R. S.; Kometani, J. M.; Reichmanis, E. *J. Vac. Sci. Technol., B* **1998**, *16*, 3716.
(6) Okoroanyanwu, U.; Byers, J.; Shimokawa, T.; Willson, C. G. *Chem. Mater.* **1998**, *10*, 3328.
(7) Ito, H. *Solid State Technol.* **1996**, *36* (7), 164.
(8) Willson, C. G. In *Introduction to Microlithography*, 2nd ed.; Thompson, L. F., Willson, C. G., Bowden, M. J., Eds.; ACS Professional Reference Book; American Chemical Society: Washington, DC, 1994; Chapter 3.
(9) Kunz, R. R.; Allen, R. D.; Wallraff, G. M. *Polym. Prepr. (Am. Chem. Soc., Div. Polym. Chem.)* **1994**, *35* (2), 939.
(10) Allen, R. D.; Wallraff, G. M.; Hofer, D. C.; Kunz, R. R. *IBM J. Res. Dev.* **1997**, *41*, 95.
(11) Nonogaki, S.; Ueno, T.; Ito, T. Chemistry of Photoresist Materials. In *Microlithography Fundamentals in Sumiconductor Devices and Fabrication Technology*; Marcel Dekker: New York, 1999; pp 115—119.
(12) Wallraff, G. M.; Hinsberg, W. D. *Chem. Rev.* **1999**, *99*, 1801.
(13) Allen, R. D.; Wallraff, G. M.; Hinsberg, W. D.; Simpson, L. L. *J. Vac. Sci. Technol., B* **1991**, *9*, 3357.
(14) Wallow, T. I.; Brock, P. J.; Dipietro, R. A.; Allen, R. D.; Opitz, J.; Sooriyakumaran, R.; Hofer, D. C.; Meute, J.; Byers, J. D.; Rich, G. K.; McCallum, M.; Schuetze, S.; Jayaraman, S.; Hullihen, K.; Vicari, R.; Rhodes, L. F.; Goodall, B. L.; Shick, R. A. *Proc. SPIE—Int. Soc. Opt. Eng.* **1998**, *3333*, 92.
(15) Gokhan, H.; Esho, S.; Ohnishi, Y. *J. Electrochem. Soc.* **1983**, *130*, 143.
(16) Kaimoto, Y.; Nozaki, K.; Takechi, M.; Abe, N. *Proc. SPIE—Int. Soc. Opt. Eng.* **1992**, *1672*, 66.
(17) Nozaki, K.; Kaimoto, Y.; Takahashi, M.; Takechi, Abe, N. *Chem. Mater.* **1994**, *6*, 1492.
(18) Takechi, S.; Takahashi, M.; Kotachi, A.; Nozaki, K.; Yano, E.; Hanyu, I. *J. Photopolym. Sci. Technol.* **1996**, *9*, 475.
(19) Yamashita, K.; Endo, M.; Sasago, M.; Nomura, N.; Nagano, H.; Mizuguchi, S.; Ono, T.; Sato, T. *J. Vac. Sci. Technol., B* **1993**, *11*, 2692.
(20) Nakano, K.; Maeda, K.; Iwasa, S.; Yano, J.; Ogura, Y.; Hasegawa, E. *Proc. SPIE—Int. Soc. Opt. Eng.* **1994**, *2195*, 194.
(21) Maeda, K.; Nakano, K.; Ohfuji, T.; Hasegawa, E. *Proc. SPIE—Int. Soc. Opt. Eng.* **1996**, *2724*, 377.
(22) Allen, R. D.; Wallraff, G. M.; DiPietro, R. A.; Hofer, D. C.; Kunz, R. R. *J. Photopolym. Sci. Technol.* **1994**, *7*, 507.
(23) Okoroanyanwu, U.; Shimokawa, T.; Byers, J.; Medeiros, D.; Willson, C. G.; Niu, Q, J.; Fréchet, J. M. J.; Allen, R. D. *Proc. SPIE—Int. Soc. Opt. Eng.* **1997**, *3049*, 92.
(24) Okoroanyanwu, U.; Shimokawa, T.; Byers, J.; Willson, C. G. *Chem. Mater.* **1998**, *10*, 3319.
(25) Nozaki, K.; Yano, E. *J. Photopolym. Sci. Technol.* **1997**, *10*, 545.
(26) Patterson, K.; Okoroanyanwu, U.; Shimokawa, T.; Cho, S.; Byers, J.; Willson, C. G. *Proc. SPIE—Int. Soc. Opt. Eng.* **1998**, *3333*, 425.
(27) Wallow, T. I.; Houlihan, F. M.; Nalamasu, O.; Chandross, E. A.; Neenan, T. X.; Reichmanis, E. *Proc. SPIE—Int. Soc. Opt. Eng.* **1996**, *2724*, 355.
(28) Houlihan, F. M.; Wallow, T. I.; Nalamasu, O.; Reichmanis, E. *Macromolecules* **1997**, *30*, 6517.
(29) Patterson, K.; Yamchika, M.; Cho, S.; Rager, T.; Yamada, S.; Byers, J.; Willson, C. G. *Polym. Mater. Sci. Eng.* **1999**, *81*, 43.
(30) Gabor, A. H.; Dimov, O.; Medina, A. N.; Bowden, M. J.; Neisser, M. O.; Houlihan, F. M.; Cirelli, R. A.; Dabbagh, G.; Hutton, R. S.; Rushkin, I. L.; Sweeney, J. R.; Nalamasu, O.; Reichmanis, E. *Polym. Mater. Sci. Eng.* **1999**, *81*, 41.
(31) Allen, R. D.; Sooriyakumaran, R.; Opitz, J.; Wallraff, G. M.; DiPietro, R. A.; Breyta, G.; Hofer, D. C. *Proc. SPIE—Int. Soc. Opt. Eng.* **1996**, *2724*, 334.
(32) Allen, R. D.; Opitz, J.; Wallow, T. I.; DiPietro, R. A.; Hofer, D. C.; Jayaraman, S.; Hullihan, K. A.; Rhodes, L. F.; Goodall, B. L.; Shick, R. A. *Proc. SPIE—Int. Soc. Opt. Eng.* **1998**, *3333*, 463.
(33) Opitz, J.; Allen, R. D.; Wallow, T. I.; Wallraff, G. M.; Hofer, D. C. *Proc. SPIE—Int. Soc. Opt. Eng.* **1998**, *3333*, 571.
(34) Koch, V. R.; Gleicer, G. J. *J. Am. Chem. Soc.* **1971**, *93*, 1657.
(35) Pasquale, A. J.; Allen, R. D.; Long, T. E. In *Forefront of Lithographic Materials Research: Proceedings of the 12th International Conference on Photopolymers*; Ito, H., Khojasteh, M. M., Li, W., Eds.; Society of Plastics Engineers (SPE): New York, pp 291—297.
(36) Pasquale, A. J.; Truong, H.; Allen, R. D.; Long, T. E. *J. Adhes.*, in press.
(37) Ito, H.; Miller, D.; Sveum, N.; Sherwood, M. *J. Polym. Sci., Part A: Polym. Chem.* **2000**, *38*, 3521.
(38) Ito, H.; Miller, D.; Sherwood, M. *J. Photopolym. Sci. Technol.* **2000**, *13*, 559.
(39) Storey, R. F.; Donnalley, A. B.; Maggio, T. L. *Macromolecules* **1998**, *31*, 1523.
(40) Pasquale, A. J.; Long, T. E. *Macromolecules* **1999**, *32*, 7954.
(41) Pasquale, A. J.; Long, T. E. *Polym. Prepr. (Am. Chem. Soc., Div. Polym. Chem.)* **2000**, *41* (1), 944.
(42) Pasquale, A. J.; Long, T. E. *J. Polym. Sci., Part A: Polym. Chem.* **2001**, *39*, 216.
(43) Hennis, A. D.; Sen, A. *Polym. Prepr. (Am. Chem. Soc., Div. Polym. Chem.)* **2000**, *41* (2), 1933.
(44) *Polymer Handbook*, 4th ed.; Brandrup, J., Immergut, E. H., Grulke, E. A., Eds.; Wiley & Sons: New York, 1999.

MA010257X